High-speed etching of SiO_2 using a remote-type pin-to-plate dielectric barrier discharge at atmospheric pressure

J. Phys. D: Appl. Phys. **43** (2010) 425207 (6pp) doi:10.1088/0022-3727/43/42/425207

High-speed etching of SiO_2 using a remote-type pin-to-plate dielectric barrier discharge at atmospheric pressure

Jong Sik Oh[1], Jae Beom Park[2], Elly Gil[1] and Geun Young Yeom[1,2]

[1] Department of Advanced Materials Science and Engineering, Sungkyunkwan University, Suwon, Kyunggi-do 440-746, Korea
[2] SKKU Advanced Institute of Nano Technology (SAINT), Sungkyunkwan University, Suwon, Kyunggi-do 440-746, Korea

E-mail: gyyeom@skk.edu

Received 11 June 2010, in final form 21 August 2010
Published 7 October 2010
Online at stacks.iop.org/JPhysD/43/425207

Abstract
High speed etching of SiO_2 has been investigated using a remote-type dielectric barrier discharge (DBD) in-line system with a multi-pin-to-plate power electrode configuration as functions of N_2/NF_3 gas combination, added gases and operating frequency of a pulse power supply. The SiO_2 etch rate increased with an increase in NF_3 flow rate (0.2–1.0 slm) in N_2 (60 slm)/NF_3 but showed a maximum with an increase in N_2 (30–80 slm) at 60 slm in the N_2/NF_3 (1 slm) gas mixture. The SiO_2 etch rate was also increased with the addition of up to 0.6 slm of He or Ar gas and it was also related to the increase in fluorine atomic density in the plasma. The addition of He or Ar to the N_2 (60 slm)/NF_3 (1 slm) and the increase in the frequency of the pulse power increased the fluorine atomic density through the increased Penning ionization/dissociation and the increased ionization by the increased pulse-on time, respectively.

1. Introduction

For various electronic devices such as microelectromechanical system (MEMS) devices, thin film transistor-liquid crystal display (TFT-LCD) devices and flexible display devices, dielectric thin film materials such as SiO_2 and Si_3N_4 are used and the patterning of those materials is carried out using wet etching or plasma etching [1–5]. The wet etching process can be done at a low cost but it shows problems such as the difficulty in fine line patterning, the difficulty in the etch endpoint detection, environmental pollution and the difficulty of in-line processing [6, 7]. Therefore, these days, most of the etch processes are carried out by plasma etching in a vacuum system. The low-pressure plasma etching process can resolve most of the problems caused by wet etching but, instead, it raises other problems such as high cost of equipment and the difficulty in manufacturing larger plasma systems to accommodate larger area substrates for display devices.

As a possible solution to the problems of low-pressure plasma etching while resolving the problems of wet etching, atmospheric pressure plasma processing systems, which can generate plasmas at atmospheric pressure without using an expensive vacuum system, have been studied [8–10]. Among the various atmospheric pressure plasma sources, a dielectric barrier discharge (DBD) plasma has been studied most widely because it is easily expandable to a larger size and easier to generate a stable DBD in the glow regime [11–15]. In addition, to reduce the possible damage of the samples by arching, high energy bombardment, thermal energy, etc during the processing, a remote-type plasma system has been investigated [16, 17]. Previously, for remote atmospheric pressure plasma systems, SiO_2 etching has been investigated by Iwasaki *et al* using a microwave discharge and by Yamakawa *et al* using a DBD [18, 19]. Even though they obtained high etch rates of SiO_2 for stationary systems, for their application in flat panel displays and/or flexible displays, the in-line system and/or roll-to-roll system need to be utilized. Also, in order to substitute conventional processes carried out by a low-pressure plasma etching system or by a wet etching system and to maximize the advantage of an atmospheric pressure plasma, a large area atmospheric pressure plasma system which has a high plasma density over the source area and which can be operated as an in-line or roll-to-roll system needs to be developed.

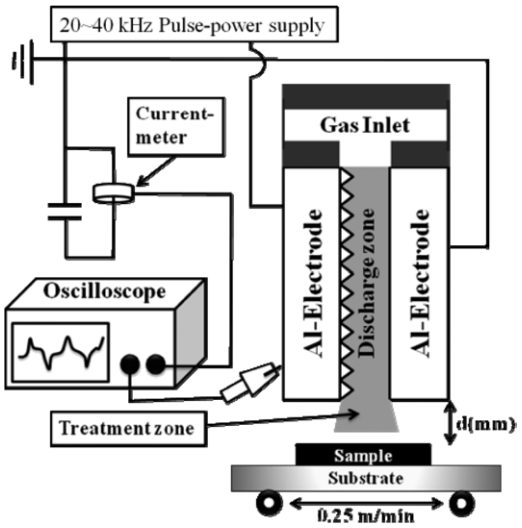

Figure 1. Schematic diagram of the remote-type modified DBD in-line system used in this experiment.

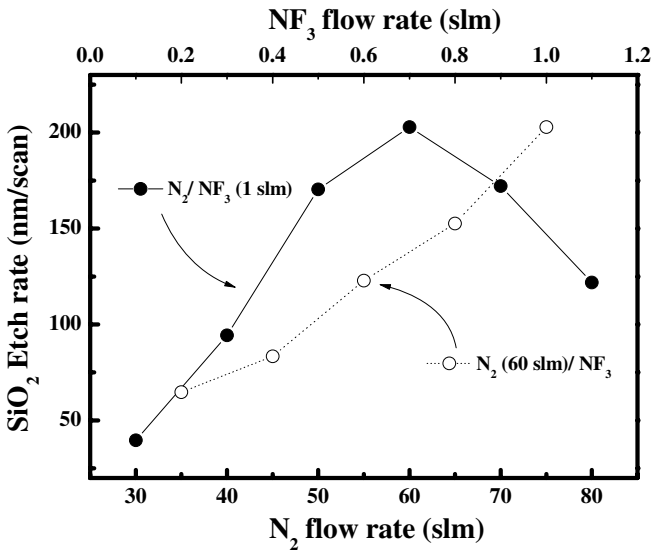

Figure 2. SiO_2 etch rate (nm/scan) measured as a function of N_2 gas flow rate and NF_3 gas flow rate for the gas combination of N_2/NF_3. The operating frequency was kept at 40 kHz (the duty time of the pulse signal was 3.5 μs) and, at this operating frequency, about 3 kW of pulse power was delivered to the source.

In this experiment, for a high density atmospheric pressure plasma system, a modified DBD with a multi-pin-to-plate power electrode configuration has been used [20, 21] and its SiO_2 etch characteristics were investigated in its application to flat panel and/or flexible display device processing. The DBD source was operated as a remote type to remove any possible damage to the substrates. And, to be applicable to in-line or roll-to-roll processing for FPD devices or flexible display devices, the samples were moved at a constant speed during the processing and the possibility of using the in-line atmospheric pressure plasma system on the patterning of SiO_2 thin films has been investigated by varying gas combination and operating frequency.

2. Experimental setup

Figure 1 shows a schematic diagram of the remote plasma-type pin-to-plate DBD used in the experiment. The discharge source consisted of a power electrode having machined pyramid-shaped multi-pins (the height of the apex and the length of the base edge of the pyramid were 1 mm and 2 mm, respectively) and a blank planar ground electrode facing each other, and the source was located vertically above the substrate for the remote-type operation (the gap between the electrodes of the remote-type DBD is 1.5 mm and the distance between the DBD source and the substrate is 2 mm). The size of the electrodes was 50 × 300 mm^2 and both electrodes were made of aluminium coated with alumina as a dielectric barrier. The power electrode was connected to a pulse power generator with a frequency in the range 20–40 kHz and a maximum applied power of 4 kW. In order to observe electrical parameters such as output voltage and consumed power, a high voltage (HV) probe and a current meter were connected to the power electrode and the ground electrode.

The etching gas consisted of a gas mixture of N_2 (30–80 slm)/NF_3 (0.2–1.0 slm) with additive gases (He, Ar, O_2)/(0.2–1.0 slm). N_2 gas was used as the discharge gas and NF_3 was used as the reactive gas. The SiO_2 samples, which were thermally grown on silicon wafers, were located 2 mm below the remote-type DBD source and the samples were moved along the substrate holder with a speed of 0.25 m min^{-1}. The remote-type plasma DBD system and the substrate holder were installed in a transparent plastic box for a controlled gas environment, and the residual gas was removed using an exhaust fan installed in the box.

The SiO_2 etch rate was estimated by measuring the etching depth with a step profilometer (TENCOR, Alpha-step 500). The voltage and consumed power were measured using an oscilloscope (Tektronics, Oscilloscope TDS 744A), a HV probe and a current meter. An optical emission spectroscope (OES) (PCM 420, SC-Technology) was located below the DBD source and was used to detect the optical emission intensities from the radicals or activated species in the plasma. The SiO_2 etch profile before/after the etching was observed by field-emission scanning electron microscopy (FE-SEM; Hitachi S-4700). The chemical bonding state of the etched silicon dioxide surface was examined by x-ray photoelectron spectroscopy (XPS) (Thermo VG SIGMA PROBE).

3. Results and discussion

Figure 2 shows the SiO_2 etch rate (nm/scan) measured as a function of N_2 gas flow rate and NF_3 gas flow rate for the gas combination of N_2/NF_3. When the NF_3 gas flow rate was varied from 0.2 to 1.0 slm, the N_2 gas flow rate was maintained at 60 slm and, when the N_2 flow rate was varied from 30 to 80 slm, the NF_3 flow rate was maintained at 1 slm. The operating frequency was kept at 40 kHz (duty time of the pulse signal was 3.5 μs), and at this operating frequency, about 3 kW of pulse power was delivered to the source. The substrate was moved at a speed of 0.25 m min^{-1}. As shown in figure 2, the increase in NF_3 flow rate from 0.2 to 1.0 slm at a fixed N_2 flow rate of 60 slm increased the SiO_2 etch rate continuously from

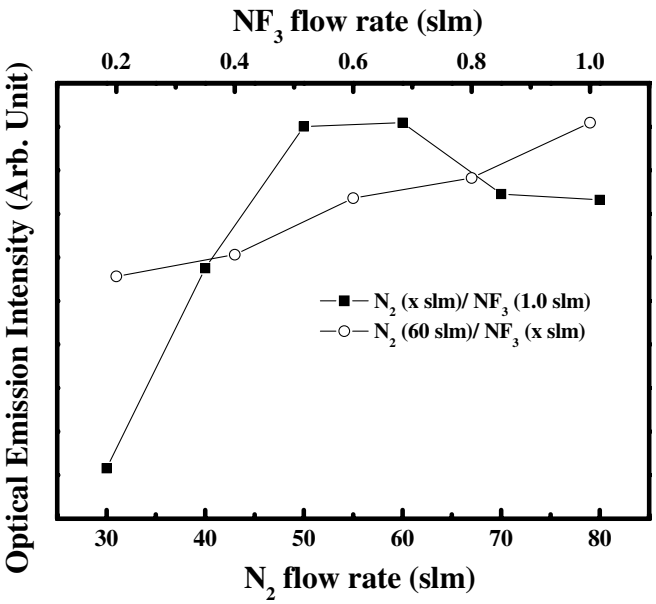

Figure 3. Fluorine atomic optical emission peak (703.9 nm) in the remote plasma source measured by OES as functions of NF_3 and N_2 flow rate in the N_2/NF_3 gas mixtures under the etch condition in figure 2.

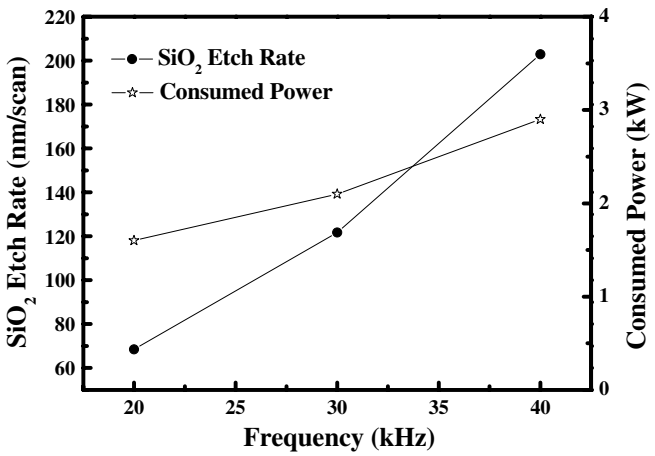

Figure 4. Effect of operating frequency on the SiO_2 etch rate. The gas combination was N_2 (60 slm)/NF_3 (1 slm) and the operating pulse voltage was about 7 kV and the pulse duration per pulse was 3.5 μs.

39.7 to 202.9 nm/scan. However, when the N_2 flow rate was varied from 30 to 80 slm with the NF_3 flow rate fixed at 1 slm, the SiO_2 etch rate was increased initially with the increase in N_2 flow rate and showed a maximum at about 60 slm of N_2 flow rate. A further increase in N_2 flow rate decreased the SiO_2 etch rate significantly. The variation of etch rate with N_2 flow rate is caused by the characteristics of the remote-type plasma system used in the experiment. With the increase in N_2 gas flow rate, more dissociated species are available on the substrate surface due to the decreased recombination of the dissociated species during the transportation to the surface; therefore, the etch rate is increased with the initial increase in N_2 gas flow rate. However, if the gas flow rate is very high, the density of the species decomposed in the remote-type plasma source is decreased due to the decreased residence time of the feed gas in the remote source; therefore, the etch rate is decreased.

For the etching of SiO_2 with N_2/NF_3 gas mixtures in a remote-type plasma system, it is impossible to enhance SiO_2 etching by ion bombardment due to the separation between the plasma source and the substrate [22]. And, in particular, for the atmospheric pressure plasma system, due to the extremely small mean free path, only a reactive fluorine atom delivered to the sample by the gas flow without volume recombination is believed to participate in the etching of SiO_2 by forming SiF_x. OES was carried out to observe the fluorine atomic optical emission peak in the remote plasma source as functions of NF_3 and N_2 flow rate in the N_2/NF_3 gas mixtures under the etch conditions in figure 2 and the results are shown in figure 3. The optical emission peak observed at 703.9 nm was used for the fluorine atomic emission peak [23]. As shown in figure 3, the increase in NF_3 flow rate at a fixed N_2 flow rate increased the fluorine optical emission peak intensity constantly similar to the SiO_2 etch rate variation observed in figure 2. Also, the increase in N_2 flow rate showed a maximum at 50–60 slm of N_2 flow rate similar to that of etch rate measured as a function of N_2 flow rate in figure 2. The increase in SiO_2 etch rate observed with the increase in NF_3 flow rate in N_2/NF_3 is believed to be related to the increase in fluorine atoms in the plasma by the increased dissociation of NF_3 with the increase in NF_3 flow rate in the gas mixture. In the case of variation of N_2 flow rate in N_2/NF_3, due to the significant variation of total gas flow rate and the volume recombination time of the reactive fluorine atom generated at the remote plasma source, the number of fluorine atoms remaining on the sample surface after the recombination during the transport from the source to the sample surface could affect the SiO_2 etch rate. The similarity of the SiO_2 etch rate variation measured as a function of N_2 flow rate to that of fluorine optical emission intensity measured as a function of N_2 flow rate appears to suggest that the fluorine atoms are not significantly recombined during the transport from the plasma source to the sample surface and the SiO_2 etch rate with N_2 flow rate is more affected by fluorine generation in the discharge source. The variation of fluorine atoms in the source with N_2 flow rate is from the variation of the NF_3 dissociation and, in general, a higher dissociation is obtained at a higher plasma density if the electron energy distribution is not changed significantly. Therefore, it is believed that the highest fluorine atomic density at 50–60 slm of N_2 gas flow rate is related to the highest plasma density at those gas flow rates.

The frequency of the operating pulse power supply was varied from 20 to 40 kHz and the effect of the operating frequency on the SiO_2 etch rate was measured and the results are shown in figure 4. The gas combination of N_2 (60 slm)/NF_3 (1 slm) was used. The voltage of the pulse was maintained at about 7 kV and the duration of each pulse was kept at 3.5 μs. In figure 4, the power consumed by the plasma is also shown. As shown in the figure, the increase in operating pulse frequency increased the SiO_2 etch rate from 68.5 to 202.9 nm/scan. The measured consumed power was also increased from 1.6 to 2.9 kW with the increase in operating frequency from 20 to 40 kHz. It is believed that the plasma is turned off during each

pulse cycle even though the positive/negative charges remain accumulated on the dielectric surface of each electrode during the pulse-off period of each pulse. The increase in pulse frequency while maintaining the pulse-on duration at each pulse increases the plasma-on time and it increases the time-averaged discharge current, which increases the consumed power to the plasma. Therefore, not only the time-averaged plasma density but also the dissociated species, such as fluorine atom, are increased with the increase in operating pulse frequency [24, 25]. Therefore, by using a higher pulse frequency at a given pulse signal, it is believed that a higher SiO_2 etch rate could be obtained by increasing the consumed power while maintaining the glow discharge-type plasma. (When ac high voltage is used, due to the variation of voltage, it is difficult to operate the plasma without the formation of a filamentary discharge particularly at a high ac power, in general. However, our experience with the pulse power supply showed that, when the pulse power is used, glow-type discharges appeared to be maintained even at higher powers possibly due to the fixed voltage and fixed pulse duration which limit the formation of a filamentary discharge.)

Additive gases such as He, Ar, and O_2 were added to N_2 (60 slm)/NF_3(1 slm) and the effect of additive gas on the SiO_2 etch rate was investigated and the results are shown in figure 5(*a*) for SiO_2 etch rate measured as functions of additive gas flow rate from 0 to 1 slm. The operating pulse frequency was kept at 40 kHz. As shown in figure 5(*a*), the increase in He and Ar flow rate up to 0.6 slm increased the SiO_2 etch rate by showing 323.4 nm/scan and 225.4 nm/scan, respectively; however, a further increase in the flow rate of He and Ar to 1 slm decreased the SiO_2 etch rate. In the case of O_2 addition, the increase in O_2 addition to N_2/NF_3 generally decreased the SiO_2 etch rate. Under the etch conditions investigated in figure 5(*a*), using OES, the emission intensities near the fluorine atomic emission peak position (703.9 nm) were measured for 0.6 slm of added gases and the results are shown in figure 5(*b*). As a reference, the optical emission intensity measured without the added gas is included. The optical emission intensity of F atom is proportional to both F atomic density and electron density. Therefore, the variation of the optical emission intensity is not solely related to the variation of F atomic density; however, in this experiment, the optical emission intensity was used as a relative measure of F atomic density. As shown in the figure, the relative optical emission peak intensity of fluorine measured as a function of added gas was similar to the SiO_2 etch rate measured as a function of added gas by showing the highest peak intensity for the addition of 0.6 slm of He and the lowest peak intensity for the addition of 0.6 slm of O_2. Therefore, the SiO_2 etch rate measured as a function of added gases is believed to be related to the change in optical emission intensity of fluorine, and therefore, possibly to the change in dissociated fluorine atoms in the plasma.

The increase in dissociated fluorine with the increase in added He and Ar up to 0.6 slm appears to be related to the increased ionization/dissociation through the Penning ionization/dissociation by the added He or Ar through the following reactions even though the dissociative ionization energy of NF_3 by electron impact is known to be nearly zero

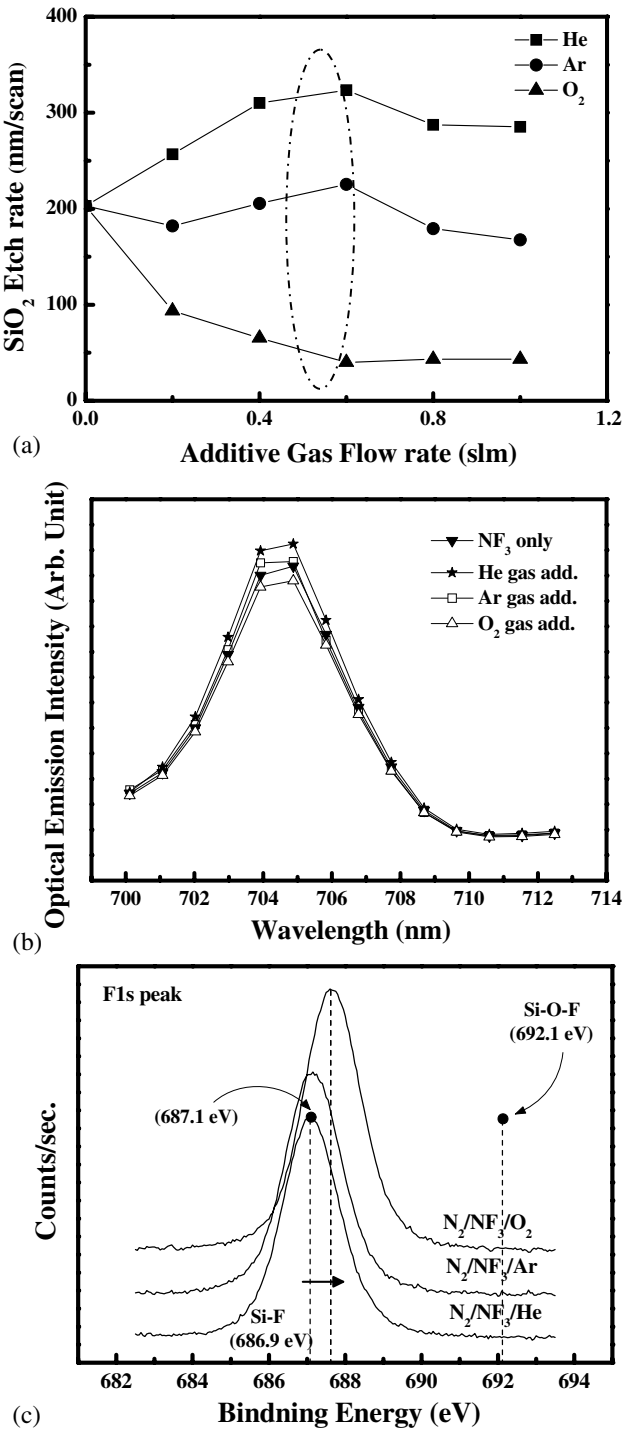

Figure 5. (*a*) Effect of additive gas flow rate (He, Ar, O_2: 0.2–1.0 slm) to N_2 (60 slm)/NF_3 (1 slm) gas mixture on the SiO_2 etch rate. The input pulse frequency was 40 kHz and the consumed power was about 3 kW. (*b*) OES of fluorine atomic peak obtained from the plasma generated with N_2 (60 slm)/NF_3 (1 slm) gas mixture and He, Ar, O_2 (0.6 slm) addition. (*c*) F1s XPS spectra on the SiO_2 surface after etching in N_2 (60 slm)/NF_3 (1 slm) with gas addition (He, Ar, O_2: 0.6 slm).

(e.g. from B E E Kastenmeier *et al*) [17]

$$He(Ar) + e \rightarrow He^*(Ar^*) + e, \quad (1)$$

$$He^*(Ar^*) + NF_3 \rightarrow He(Ar) + NF_3^*/He(Ar) + NF_3^+ + e, \quad (2)$$

$$NF_3^* \rightarrow NF_2 + F, \quad (3)$$

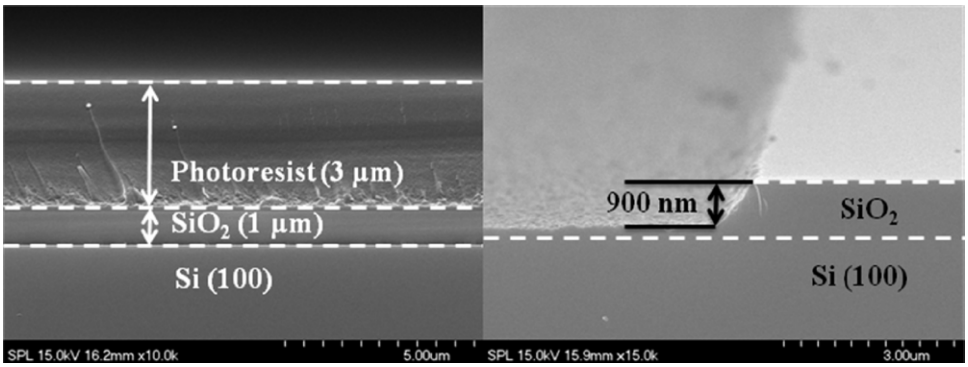

Figure 6. SEM micrograph observed before/after the etching of 1 μm thick SiO_2 on silicon with N_2 (60 slm)/He (0.6 slm)/NF_3 (1 slm) and at about 3 kW of 40 kHz pulse power. The sample was scanned three times at a speed of 0.25 m min^{-1}.

where the formation energies of the metastable species for He and Ar in equation (1) are 19.8 eV and 11.6 eV, respectively. The formation energy of NF_3^* in equation (2) is known to be 8.3 eV (while the ionization energy for NF_3 in equation (2) is about 13.2 eV [27]), and due to the higher energy state of He* metastables compared with Ar* metastables, a higher density of NF_3^* excited states is expected. The dissociation of NF_3^* into NF_2 and F occurs spontaneously because the binding energy of NF_2–F is in the range 2.5–3.2 eV (2.5 eV [26], 3.2 eV [28], 2.6 eV [29]). Therefore, higher dissociated fluorine obtained by He compared with Ar is believed to be related to the higher potential of He* metastables compared with that of Ar* metastables. However, the decrease in SiO_2 etch rate for He or Ar higher than 0.6 slm appears to be related to the decrease in fluorine atomic density on the SiO_2 surface due to the decrease in NF_3 partial pressure with the increase in added gas flow rate. In the case of O_2 addition, due to the high electronegativity of oxygen, [30] fluorine dissociation was decreased by the decreased ionization with an increase in oxygen addition by showing a lower optical emission intensity of fluorine as shown in figure 5(*b*), that is, possibly by showing a lower fluorine atomic density. The surface of SiO_2 etched with different added gases was examined with XPS and the F1s binding energy peaks on the etched SiO_2 surface are shown in figure 5(*c*). As shown in the figure, for the addition of He or Ar, the F1s peak was located at 687.1 eV close to the Si–F bonding peak (686.9 eV) indicating the possible formation of volatile SiF_x for SiO_2 etching. However, when oxygen was added, the F1s peak was shifted to a higher binding energy (692.1 eV) which might suggest the formation of Si–O–F bonding and cause a decrease in the SiO_2 etching by preventing the formation of volatile SiF_x [31, 32]. Therefore, the decease in SiO_2 etch rate with the addition of oxygen to N_2/NF_3 was related not only to the decrease in plasma density in the plasma source but also to the formation of Si–O–F bonding on the surface.

Figure 6 shows the SEM micrographs observed before/after the etching of 1 μm thick SiO_2 on silicon. Etching was carried out with N_2 (60 slm)/He (0.6 slm)/NF_3 (1 slm) and at about 3 kW of 40 kHz pulse power. The sample was scanned at a speed of 0.25 m min^{-1}. As shown in figure 6, after scanning the sample for three times while operating the plasma source under the above condition, a SiO_2 etch depth of about 900 mm could be observed.

4. Conclusions

In this study, a remote-type modified DBD in-line system with a multi-pin-to-plate power electrode configuration has been used and its SiO_2 etch characteristics were investigated as functions of N_2/NF_3 gas combination, added gases (He, Ar and O_2) and the operating frequency of a pulse power. The SiO_2 etch rate measured as a function of N_2 flow rate in N_2/NF_3 (1 slm) showed a maximum at about 60 slm of N_2 flow rate, which was related to the highest fluorine density in the plasma due to the highest plasma density in the gas mixture of N_2 (60 slm)/NF_3 (1 slm). When He, Ar and oxygen were added to N_2 (60 slm)/NF_3 (1 slm), a further increase in SiO_2 etch rate could be observed for the addition of He and Ar due to the increase in fluorine atomic density in the plasma through the Penning ionization/dissociation caused by He and Ar ions. In the case of oxygen addition, due to the high electronegativity of oxygen, which decreases the plasma density, and due to the formation of Si–O–F bonding on the SiO_2 surface, which prevents the formation of volatile SiF_x, the SiO_2 etch rate decreased with the increase in oxygen addition. When the pulse frequency was increased at a fixed voltage, due to the increase in input power without the formation of a filamentary discharge, an increase in SiO_2 etch rate could be observed for the frequency range 20–40 kHz. Under the etch condition of N_2 (60 slm)/He (0.6 slm)/NF_3 (1 slm), at about 3 kW of 40 kHz pulse power and a sample scanning speed of 0.25 m min^{-1}, a SiO_2 etch rate of about 323.4 nm/scan could be obtained.

Acknowledgments

This work was supported in part by the World Class University programme of the National Research Foundation of Korea (Grant No R32-2008-000-10124-0) and by the Ministry of Education, Science and Technology (2010-0015035). This work was also supported by the Korea Industrial Technology Foundation (KOTEF) through the Human Resource Training Project for Strategic Technology.

References

[1] Paul A K, Dimri A K and Bajpai R P 2003 *Vacuum* **68** 191
[2] Sekine M 2002 *Appl. Surf. Sci.* **192** 270

[3] Tsai W, Mueller G, Lindquist R, Frazier B and Vahedi V 1996 *J. Vac. Sci. Technol.* B **14** 3276
[4] Baram A and Naftali M 2006 *J. Micromech. Microeng.* **16** 2287
[5] Ni H, Lee H J and Ramirez A G 2005 *Sensors Actuators* A **119** 553
[6] Iliescu C, Chen B and Miao J 2008 *Sensors Actuators* A **143** 154
[7] Brugger J, Beljakovic G, Despont M, Biebuyck H, de Rooij N F and Vettiger P 1998 *Sensors Actuators* A **70** 191
[8] Tendero C, Tixier C, Tristant P, Desmaison J and Leprince P 2006 *Spectrochim. Acta* B **61** 2
[9] Park J Y, Henins I, Herrmann H W, Selwyn G S, Jeong J Y, Hicks R F, Shim D and Chang C S 2000 *Appl. Phys. Lett.* **76** 288
[10] Schäutze A, Jeong J Y, Babayan S E, Park J Y, Selwyn G S and Hicks R F 1998 *IEEE Trans. Plasma Sci.* **26** 1685
[11] Lee Y H, Kyung S J, Jeong C H and Yeom G Y 2005 *Japan. J. Appl. Phys.* **44** L78
[12] Kogelschatz U 2003 *Plasma Chem. Plasma Process.* **23** 1
[13] Okazaki S and Kogoma M 1993 *J. Photopolym. Sci. Technol.* **6** 339
[14] Massines F, Rabehi A, Decomps P, Gadri R B, Segur P and Mayoux C 1998 *J. Appl. Phys.* **83** 2950
[15] Fridman G, Shereshevsky A, Jost M M, Brooks A D, Fridman A, Gutsol A, Vasilets V and Friedman G 2007 *Plasma Chem. Plasma Process.* **27** 163
[16] Nowling G R, Babayan S E, Jankovic V and Hicks R F 2002 *Plasma Sources Sci. Technol.* **11** 97
[17] Kastenmeier B E E, Matsuo P J, Oehrlein G S and Langan J G 1998 *J. Vac. Sci. Technol.* A **16** 2047
[18] Iwasaki M, Ito M, Uehara T, Nakamura M and Hori M 2006 *J. Appl. Phys.* **100** 093304
[19] Yamakawa K, Hori M, Goto T, Den S, Katagiri T and Kano H 2004 *Appl. Phys. Lett.* **85** 549
[20] Vertriest R, Morent R, Dewulf J, Leys C and Langenhove H V 2003 *Plasma Sources Sci. Technol.* **12** 412
[21] Lee Y H and Yeom G Y 2005 *J. Korean Phys. Soc.* **47** 74
[22] Park J B, Kyung S J and Yeom G Y 2008 *J. Appl. Phys.* **104** 083302
[23] Campo A, Cardinaud Ch and Turban G 1995 *Plasma Sources Sci. Technol.* **4** 398
[24] Kyung S J, Park J B, Lee Y H, Lee J H and Yeom G Y 2007 *Surf. Coat. Technol.* **202** 1204
[25] Park J Y, Henins I, Herrmann H W, Selwyn G S and Hicks R F 2001 *J. Appl. Phys.* **89** 20
[26] Stalder K R and Vidmar R J 1997 *Plasma Sources Sci. Technol.* **6** 461
[27] Massines F, Sègur P, Gherardi N, Khamphan C and Ricard A 2003 *Surf. Coat. Technol.* **174–175** 8
[28] Reese R M and Dibeler V H 1956 *J. Chem. Phys.* **24** 1175
[29] Donnelly V M, Flamm D L, Dautremont-Smith W C and Werder D J 1984 *J. Appl. Phys.* **55** 1
[30] Park J B, Kyung S J and Yeom G Y 2007 *Japan. J. Appl. Phys.* **46** L942
[31] Park H H, Kwon K H, Lee S H, Koak B H, Nahm S, Lee H T, Cho K I, Kwon O J and Kang Y I 1994 *ETRI J.* **16** 45
[32] Demyanova L P and Tressaud A 2009 *J. Fluorine Chem.* **130** 799